MRI in Pre-Clinical Models of Muscle Disease

Bruce M. Damon, PhD
Vanderbilt University, Nashville TN USA

I. Introduction

This work describes the use of MRI to characterize skeletal muscle damage and repair processes in pre-clinical animal models. We begin with a description of the rationale for these studies. We then move on to a brief description of healthy skeletal muscle structure, followed by an overview of the processes of muscle damage and repair. We then describe selected small animals of muscle damage and repair, followed by a survey of MRI studies using these models. We focus on two specific MRI methods, transverse relaxometry and diffusion imaging. We conclude with some brief remarks.

II. Rationale for Pre-Clinical MRI Studies of Muscle Disease

Pre-clinical MRI studies of muscle disease are used for several reasons. One application is the development of image-based biomarkers for muscle damage and repair, under the hypothesis that they will provide additional, more specific, and/or less invasive markers of disease than existing approaches such as muscle biopsy or measuring the serum concentrations of enzymes such as creatine kinase (CK). The difficulties with these measurements are that CK levels are not well correlated with muscle damage (1) and biopsies induce additional muscle damage and are subject to sampling errors. Another application for pre-clinical MRI in muscle disease is to develop an improved understanding of disease pathology and/or mechanism. MRI offers a large range of structural and functional measurement possibilities; also, MRI data can be integrated with those from other imaging modalities, providing for a broad characterization of disease processes. Finally, MRI is applicable in studies of candidate drug efficacy, the mechanism of drug action, or in monitoring therapeutic response to other interventions. With regard to these last two applications, it is noteworthy that the non-invasive, non-destructive nature of MRI makes it a good choice for repeated studies in the same animal; the benefits of this approach include reduced animal use, reduced biological variability, and the addition of new insights into disease mechanisms and/or therapeutic effect that comes from the use of a longitudinal design.

III. Structural, Physiological, and Biochemical Features of Healthy Muscle

We begin with an abbreviated description of skeletal muscle structure. The cells of skeletal muscles are referred to as fibers, which have an elongated, generally cylindrical shape and multiple, peripherally located nuclei. Skeletal muscle cells are up to tens of cm long and have diameters of 30-80 μm. Most of a fiber's volume is occupied by the contractile protein filaments (myofibrils) and surrounding water. The myofibrils are arranged parallel to the longitudinal axis of the fiber and contain contractile proteins (actin and myosin), regulatory proteins (such as troponin and tropomyosin), and structural proteins (such as titin, nebulin, and C protein). The smallest functional unit of contraction is the sarcomere; myofibrils consist of a large number of sarcomeres in series. The structure at the junction between two serially arranged sarcomeres is called the Z-disc. The myofibrils are linked to membrane-associated protein complexes by the intermediate filaments, containing the proton desmin. Extracellular linkages then occur to the basal lamina and the endomysium, a connective tissue structure that envelops the fibers. Outside of the plasma membrane, but inside of the basal lamina, lie satellite cells (skeletal muscle stem cells).

Muscle fibers also contain the sarcoplasmic reticulum (SR). The SR has a predominantly longitudinal orientation, contains the cell's intracellular Ca^{2+} store, and plays a crucial role in muscle's activation and relaxation processes. At rest, the intracellular [Ca^{2+}] is maintained at <0.1 μM by Ca^{2+} exchangers and pumps located in the plasma and mitochondrial membranes. Muscle contraction results from a transient, ~100-fold elevation in the intracellular [Ca^{2+}], causing the actin and myosin filaments to bind and slide with respect to each other. Release of the actomysosin complex and the restoration of the intracellular ionic environment require ATP hydrolysis. During contractions, the ATP concentration is maintained by increased flux through the creatine kinase, glycolytic and oxidative phosphorylation reactions; these metabolic activities are, in turn, supported by increased blood flow.

Between the individual fibers and the whole muscle, intermediate levels of structural organization also exist. Structurally, groups of 100-200 fibers are contained with connective tissue structures called fascicles; fascicles are surrounded by perimysium and have an area of ~0.25 mm^2. The whole muscle itself is surrounded by a connective tissue structure called the epimysium.

IV. Overview of Muscle Damage and Repair Processes

Muscle damage and repair processes are generally seen to occur in four phases. The first phase is the damaging event itself, such as ischemia-reperfusion injury, infection, or lengthening under load (a so-called eccentric contraction). Many aspects of the initial damage to muscles and a muscle's responses to this damage are similar, regardless of the mechanism of injury. The remainder of this section includes a general description of those responses, presuming that the responses follow a single damaging event.

The second phase is an autogenic phase, lasting for several hours following injury. A key process during this time is a local loss of Ca^{2+} homeostasis, caused by direct injury to cell membranes, local anoxia and ATP depletion, and/or opening of stretch-sensitive Ca^{2+} channels in the cell membrane (2-5). One consequence of increased intracellular [Ca^{2+}] is that the enzyme phospholipase A_2 (PLA_2), which digests lipid membranes, is activated (6-8). This reduces membrane integrity and forms hydroxyl radicals, a type of reactive oxygen species (ROS) (9). Second, the proteases calpain 1-3 are activated (10-13). Calpains act on desmin and titin (14-16). This disrupts sarcomere alignment (so-called "Z-disk streaming"). Other consequences of the loss of Ca^{2+} homeostasis are ROS-mediated reductions in the SR Ca^{2+}-ATPase activity (9), further raising intracellular [Ca^{2+}]; stimulation of mitochondrial ROS production by PLA_2 activation (17,18); and increased mitochondrial uptake of Ca^{2+}. Mitochondrial Ca^{2+} uptake is a normal event that links increased metabolic demand to increased oxidative ATP production during contraction. In the case of muscle damage, however, excessive mitochondrial stimulation can result in ROS-mediated inner mitochondrial membrane damage and decreased ATP production (19-21). The potential exists for a vicious cycle to occur unless repair processes are activated.

The third phase of muscle damage is the phagocytic phase, beginning hours after the induction of damage and persisting for up to 4-6 days afterwards. This is a typical inflammatory response triggered by some of the digestive products of the autogenic phase (22), cytokines from damaged muscle cells (23,24), and complement components (25). Shortly after damage occurs, neutrophils are recruited to sites of muscle damage and release proteases that degrade damaged cell components (26,27); the neutrophils may also phagocytose these cell components (28). A consequence of the neutrophils' action on cellular debris is that healthy cell membranes may also be affected. Neutrophils also attract macrophages, which enter the damaged cells. The

macrophages secrete digestive enzymes and other molecules and then ingest the breakdown products. It is during this phase, 2-5 days following damage, that peak levels of subject-reported soreness and swelling occur (29). Also, plasma membrane damage allows normally intracellular enzymes such as CK, lactate dehydrogenase, and aldolase to enter the circulation. This forms the rationale for using serum CK levels as an indicator of muscle damage.

The severity of the above events may vary: either reparable local cellular damage or severe, irreparable damage to the fiber may occur. In the former case, the processes that are activated comprise the fourth phase of muscle damage and repair. The damaged portion of the fiber is sealed off by completing the plasma membrane in the two healthy bordering regions. Nearby satellite cells become activated, proliferate, differentiate into myoblasts, and fuse to form a myotube. The myotube reconnects the two healthy fiber fragments and the muscle fiber is repaired. Morphologically, muscle cells undergoing or just having undergone repair can be identified by the central, rather than peripheral, location of nuclei. In the case, of severe, irreparable muscle damage, there will be complete cellular digestion and phagocytosis; these fibers are replaced by adipose tissue, and fibrosis occurs (30).

V. Selected Small Animal Models for Human Muscle Damage and Repair

The above discussion provided a short overview of the processes of muscle damage and repair and reveals a rather complex response. It should not be surprising, however, that the pathology in *in vivo* muscle diseases occurs in a more complicated fashion still. In part, this is because damage is being induced repeatedly, and so there is an asynchronous incidence of these processes across the many fibers within a muscle. Also, interactions among body systems occur, leading to the more complex presentation and mechanism of pathology.

Animal models of human muscle disease have been developed or occur naturally in many species. For convenience, we classify these as "full" models of the human disease (intended to model all or most aspects of the disease and often sharing a similar or identical pathogenetic mechanism) and "reduced" models (intended to model a limited number of disease components, often by using a single event to induce damage to otherwise healthy muscle(s)). The advantages of the full models are that they allow studies of disease pathogenesis, therapeutic response, and biomarker utility in the most externally valid manner. The advantages of using reduced models is that in addition to simplifying the pathology, the synchronous nature of the damaging event across many fibers also provides a larger dynamic range of responses. This may allow for more robust and quantitative comparisons of MRI data with other forms of data, such as histology or laboratory findings.

There are many examples of full and reduced animal models of muscle disease. Full animal muscle disease models exist for polymyositis (31-35), Duchenne muscular dystrophy (DMD; reviewed fully in (36)), limb girdle muscular dystrophy (37,38), and other diseases. Of these, it is the genotypic model of DMD, the *mdx* mouse, that has been most studied. As reviewed by Willman *et al.* (36), the *mdx* mouse models a large number of aspects of human DMD well, including impaired muscle function, elevated CK, elevated intracellular [Ca^{2+}], central nucleated muscle fibers, and variations in cell size (with some fibers being severely atrophied and others being swollen and vacuolated). The *mdx* mouse, like DMD patients (39), also has perfusion deficits owing to the mislocalization of the neuronal form of nitric oxide synthase within the muscle fiber (40). Aspects of DMD pathology are not well modeled by the *mdx* mouse; these include fat infiltration and fibrosis, the latter of which occurs extensively only in the diaphragm of *mdx* mice. Examples of reduced models of muscle damage include lengthening contractions (41), ischemia-reperfusion injury (*e.g.*, (42,43)), or the local injection of

a toxin such as notexin (44,45) or cardiotoxin (46) or an inflammatory agent such as λ-carrageenan (47,48).

VI. MRI Studies of Small Animal Models for Human Muscle Damage and Repair

The above discussions have described the pathology associated with muscle damage and repair in general terms, and in several small animal models of human muscle disease more specifically. From this discussion, several potential targets for imaging muscle damage emerge. These include the inflammatory response and the corresponding expansion of the interstitial space, fat infiltration, damage to the cell membrane, and fibrosis. The principal techniques that have been used to study these processes in pre-clinical models include transverse relaxometry and diffusion imaging. This section describes the biophysical rationale for these measurements and presents the results of some illustrative implementations of each technique.

VI.A. Transverse Relaxometry Studies of Muscle Damage and Repair

Biophysical Basis There is a long history of using transverse relaxometry to characterize muscle tissue, both *in vivo* and *ex vivo*. Dating back to studies in the early 1970's by Belton and colleagues (49-51) and Hazlewood (52), it has been recognized that there is a multiexponential (or at least, non-monoexponential) character to transverse relaxation in *ex vivo* samples. The observations initially made were that there is a bound water pool with a T_2 <10 ms plus two free water pools: a rapidly relaxation major fraction (T_2 ~35 ms; ~90% of total tissue water proton signal) and a more slowly relaxing minor fraction (T_2 ~140 ms; ~10% of total tissue water proton signal). These free water fractions were proposed to correspond, respectively, to intracellular and interstitial water. While some debate existed initially with regard to this explanation (53), a study by Cole *et al.* (54) using tissue mimetic chemical phantoms and macerated muscle tissue definitively established that water compartmentation in *ex vivo* muscle tissue has this multiexponential character, with the structural basis just described.

Whether or not this multiexponential character exists *in vivo* has been the subject of greater debate. The fundamental issue is the rate of trans-sarcolemma water exchange and whether or not it is fast enough, given the difference in transverse relaxation rates between the intracellular and interstitial spaces, to create a single effective free water pool or two pools exchanging at a slow or intermediate rate. Several studies (48,55) have provided evidence for monoexponential relaxation in healthy mammalian muscle *in vivo* that transitions to biexponential relaxation in the presence of edema. Other authors have suggested that there are two (47) or even as many as five distinct relaxation components (56-59), the latter observations made using extremely high signal-to-noise ratio data. The exact nature of water compartmentalization in muscle tissue *in vivo* and the rates of exchange between them are issues that need to be resolved in order to understand fully the mechanisms of transverse relaxation in skeletal muscle *in vivo*. For the present discussion, however, the most salient point is that damage processes such as the loss of membrane integrity and the expansion of the interstitial space by edema will increase the T_2 of muscle water protons.

In Vivo Implementations Many reduced muscle disease models have been studied, which have helped to establish a sound basis for using T_2 measurements to localize and reflect the degree of muscle damage and to establish the pathological correlates of T_2 changes. For example, injection of λ-carrageenan into the paw (47) or muscle ((48); Figure 1) of a rodent induces a local inflammatory response that includes edema and inflammatory cell infiltration (60). Significantly elevated T_2 values in response to notexin injection have also been reported (44,46). T_2 changes, spatially correlated with histological observations, have also been observed in

response to ischemia-reperfusion injury (43); these authors observed larger T_2 responses when ischemia and electrical muscle stimulation were combined, indicating that T_2 responds in a graded fashion to damage. T_2 elevations have also been reported in mice with genetic models of muscular dystrophy, including the *mdx* mouse (61) and γ-sarcoglycan knockout mice (62). Moreover, the T_2 changes appear to be responsive to clinical interventions, such as sildenafil treatment of *mdx* mice (63) or gene replacement of γ-sarcoglycan knockout mice (62).

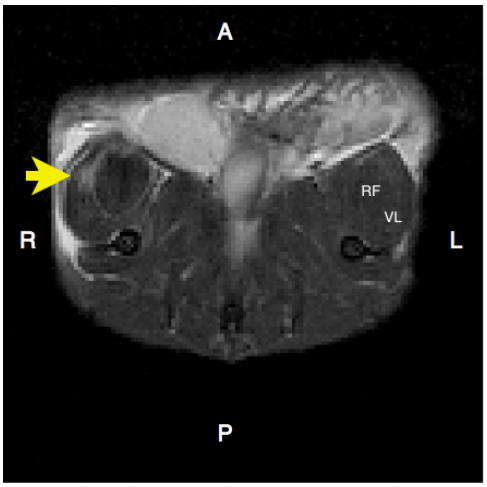

Figure 1. T_2-weighted image revealing contrast change following injection of λ-carrageenan to the right anterior thigh compartment of a C57/BlJ6 mouse reveals signal changes in the vastus lateralis (VL) and rectus femoris (RF) muscles.

VI.A. Diffusion MRI Studies of Muscle Damage

Biophysical Basis A classic study by Cleveland and colleagues revealed two important characteristics of water diffusion in muscle: first, that the diffusion coefficient is reduced from its value in free water and second, that the diffusion coefficient is greater parallel to the long axis of muscle fibers than perpendicular to the fibers' long axis (64). Because of this, characterizing water diffusion in muscle using a simple scalar quantity is inappropriate; a more complex mathematical model is required. Almost exclusively, this has been done using a three-dimensional (3D) tensor model, as described by Basser *et al.* (65). Qualitatively, the tensor model envisions diffusion as a 3D ellipsoid, with the long axis of the ellipsoid being coincident with the long axis of the muscle fiber. To form the diffusion tensor, measurements of water diffusion in six non-collinear directions must be made; the tensor can then be formed using ordinary least squares, weighted least squares, or curve fitting techniques; the relative merits of these approaches are described in Ref. (66). The tensor is then diagonalized, resulting in a diagonal matrix of eigenvalues (describing the dimensions of the ellipsoid) and three eigenvectors (describing the orientation of the ellipsoid in 3D space; stated mathematically, the eigenvector matrix describes the rotation of the muscle fibers away from the laboratory frame of reference). The largest, or first, eigenvalue (λ_1) is the diffusion coefficient along the long axis of the cell and its eigenvector (ε_1) describes the local fiber direction. The second and third eigenvalues (λ_2 and λ_3, respectively) and their eigenvectors (ε_2 and ε_3, respectively) represent diffusion perpendicular to the long axis of the cell; the three eigenvectors are constrained to be mutually orthogonal. Other values that can be derived from the diffusion tensor are the mean diffusivity and fractional anisotropy (FA). The mean diffusivity is calculated as the mean of λ_1, λ_2 and λ_3. The FA ranges between 0 and 1 and is used to describe how different λ_1, λ_2 and λ_3 are: an FA value of 0 indicates completely random and isotropic diffusion, while a value of 1 indicates diffusion in a single direction only.

The potential value of these measurements for characterizing muscle damage lies in the structural basis for the reduced and anisotropic diffusion in skeletal muscle. One fundamental source of diffusion hindrance in the transverse direction is the cell membrane itself, which has a finite permeability to water. Because of the large diameter of muscle fibers, there is a long diffusion time (up to hundreds of ms) that is required for a typical water molecule to encounter the cell membrane. For this reason, it is unlikely that the greater reduction of λ_2 and λ_3 from the

value for free water (compared to that for λ_1) is primarily due to finite membrane water permeability, at least at the short diffusion times (20-50 ms) used in most *in vivo* diffusion tensor MRI experiments (67-69). Some clues can be found, however, in the additional, monotonic reduction of transverse diffusivities as a function of increasing diffusion time (70,71). It may be that the initial reduction in transverse diffusion coefficients results from the diffusion-restricting effects of the actin- and myosin-containing filaments, which are spaced tens of nm apart in the transverse direction; the additional reduction would then result from an increasing number of encounter of water molecules with the cell membrane. The quantitative contribution of the intracellular proteins and cell membrane is an issue that needs still to be resolved. For the purposes of the present discussion, the most important point is that pathologic processes such as Z-disc streaming and membrane damage will tend to increase the transverse diffusion coefficients and decrease diffusion anisotropy. Though not discussed above, edema would be expected to produce similar changes, as the increase in interstitial water content would tend to increase the distances between cells and among the proteins of the extracellular connective tissue network.

In Vivo Implementations Diffusion imaging has been used in several muscle damage models to provide a quantitative measurement associated with muscle damage. For example, Heemskerk *et al.* (43) observed that during the reperfusion phase of ischemia-reperfusion injury, the mean diffusivity is increased, along with the T_2. When more severe damage is created by simultaneous electrical stimulation during the ischemic phase, the FA also decreased. The changes in mean diffusivity were due mainly to increases in λ_2 and λ_3, and λ_3 in particular. A subsequent study from these authors (42), using a femoral artery ligation model, further revealed different temporal and spatial patterns to the diffusion and T_2 changes, suggesting that these parameters may reflect different aspects of muscle damage and regeneration. Both of these studies provided histological data that supported the MRI observations. The λ-carrageenan injection used by Fan and Does (48) to induce edema and cause the appearance of the second T_2 component also resulted in the appearance of a second diffusion component. The second diffusion component was associated with the long T_2 component and was characterized by greater, and more isotropic, diffusion than the diffusion component associated with the short T_2 component. While diffusion in the brain of *mdx* mice has been studied (72), to date there exist only preliminary observations of water diffusion changes in full muscle disease models, such as the *mdx* mouse (73).

VII. Concluding Points

At the intracellular, cellular, and tissue/organ levels of biological complexity, skeletal muscles are highly organized and regularly structured tissues. When this order is disrupted by damage due to disease or injury, changes in MRI-observed transverse relaxation and water diffusion properties occur. While issues pertinent to the specific biological bases for T_2 and diffusion changes need to be resolved, T_2 and diffusion data have each been shown to indicate muscle damage robustly and quantitatively and to correspond to histological indices of muscle damage. As a final point, it is noted that space and time limitations preclude a full discussion of other potential MRI measures for characterizing muscle damage, such as magnetization transfer imaging (44) and/or contrast-enhanced imaging (74).

VIII. Acknowledgements

Our work in these areas has been supported by NIH grants NIH/NIAMS AR050101 and NIH/NIAMS AR050791. The author thanks his mentors, faculty colleagues, and current and former trainees for helpful discussions.

IX. References

1. Worrall JG, Phongsathorn V, Hooper RJ, Paice EW. Racial variation in serum creatine kinase unrelated to lean body mass. Br J Rheumatol 1990;29(5):371-373.
2. Fredsted A, Mikkelsen UR, Gissel H, Clausen T. Anoxia induces Ca^{2+} influx and loss of cell membrane integrity in rat extensor digitorum longus muscle. Exp Physiol 2005;90(5):703-714.
3. Gissel H. The role of Ca^{2+} in muscle cell damage. Ann N Y Acad Sci 2005;1066:166-180.
4. Guharay F, Sachs F. Stretch-activated single ion channel currents in tissue-cultured embryonic chick skeletal muscle. J Physiol 1984;352:685-701.
5. Jones DA, Jackson MJ, McPhail G, Edwards RH. Experimental mouse muscle damage: the importance of external calcium. Clin Sci (Lond) 1984;66(3):317-322.
6. Bruton JD, Lannergren J, Westerblad H. Mechanisms underlying the slow recovery of force after fatigue: importance of intracellular calcium. Acta Physiol Scand 1998;162(3):285-293.
7. Jackson MJ, Jones DA, Edwards RH. Experimental skeletal muscle damage: the nature of the calcium-activated degenerative processes. Eur J Clin Invest 1984;14(5):369-374.
8. Sandercock DA, Mitchell MA. Myopathy in broiler chickens: a role for Ca^{2+}-activated phospholipase A2? Poult Sci 2003;82(8):1307-1312.
9. Xu KY, Zweier JL, Becker LC. Hydroxyl radical inhibits sarcoplasmic reticulum Ca^{2+}-ATPase function by direct attack on the ATP binding site. Circ Res 1997;80(1):76-81.
10. Branca D, Gugliucci A, Bano D, Brini M, Carafoli E. Expression, partial purification and functional properties of themuscle-specific calpain isoform p94. Eur J Biochem 1999;265(2):839-846.
11. Diaz BG, Moldoveanu T, Kuiper MJ, Campbell RL, Davies PL. Insertion sequence 1 of muscle-specific calpain, p94, acts as an internal propeptide. J Biol Chem 2004;279(26):27656-27666.
12. Kinbara K, Sorimachi H, Ishiura S, Suzuki K. Muscle-specific calpain, p94, interacts with the extreme C-terminal region of connectin, a unique region flanked by two immunoglobulin C2 motifs. Arch Biochem Biophys 1997;342(1):99-107.
13. Sultan KR, Dittrich BT, Leisner E, Paul N, Pette D. Fiber type-specific expression of major proteolytic systems in fast- to slow-transforming rabbit muscle. Am J Physiol Cell Physiol 2001;280(2):C239-247.
14. Reddy MK, Etlinger JD, Rabinowitz M, Fischman DA, Zak R. Removal of Z-lines and alpha-actinin from isolated myofibrils by a calcium-activated neutral protease. J Biol Chem 1975;250(11):4278-4284.
15. Goll DE, Thompson VF, Li H, Wei W, Cong J. The calpain system. Physiol Rev 2003;83(3):731-801.

16. Arthur GD, Booker TS, Belcastro AN. Exercise promotes a subcellular redistribution of calcium-stimulated protease activity in striated muscle. Can J Physiol Pharmacol 1999;77(1):42-47.
17. Favero TG, Colter D, Hooper PF, Abramson JJ. Hypochlorous acid inhibits Ca^{2+}-ATPase from skeletal muscle sarcoplasmic reticulum. J Appl Physiol 1998;84(2):425-430.
18. Nethery D, Callahan LA, Stofan D, Mattera R, DiMarco A, Supinski G. PLA(2) dependence of diaphragm mitochondrial formation of reactive oxygen species. J Appl Physiol 2000;89(1):72-80.
19. Grijalba MT, Vercesi AE, Schreier S. Ca^{2+}-induced increased lipid packing and domain formation in submitochondrial particles. A possible early step in the mechanism of Ca^{2+}-stimulated generation of reactive oxygen species by the respiratory chain. Biochemistry 1999;38(40):13279-13287.
20. Crompton M, Virji S, Doyle V, Johnson N, Ward JM. The mitochondrial permeability transition pore. Biochem Soc Symp 1999;66:167-179.
21. Duchen MR. Mitochondria in health and disease: perspectives on a new mitochondrial biology. Mol Aspects Med 2004;25(4):365-451.
22. Raj DA, Booker TS, Belcastro AN. Striated muscle calcium-stimulated cysteine protease (calpain-like) activity promotes myeloperoxidase activity with exercise. Pflugers Arch 1998;435(6):804-809.
23. Ostrowski K, Rohde T, Zacho M, Asp S, Pedersen BK. Evidence that interleukin-6 is produced in human skeletal muscle during prolonged running. J Physiol 1998;508(3):949-953.
24. Suzuki K, Yamada M, Kurakake S, Okamura N, Yamaya K, Liu Q, Kudoh S, Kowatari K, Nakaji S, Sugawara K. Circulating cytokines and hormones with immunosuppressive but neutrophil-priming potentials rise after endurance exercise in humans. Eur J Appl Physiol 2000;81(4):281-287.
25. Frenette J, Cai B, Tidball JG. Complement Activation Promotes Muscle Inflammation during Modified Muscle Use. Am J Pathol 2000;156(6):2103-2110.
26. Suzuki K, Totsuka M, Nakaji S, Yamada M, Kudoh S, Liu Q, Sugawara K, Yamaya K, Sato K. Endurance exercise causes interaction among stress hormones, cytokines, neutrophil dynamics, and muscle damage. J Appl Physiol 1999;87(4):1360-1367.
27. Tidball J, Wehling-Henricks M. Damage and inflammation in muscular dystrophy: potential implications and relationships with autoimmune myositis. Current Opinion in Rheumatology 2005;17(6):707-713.
28. Lowe DA, Warren GL, Ingalls CP, Boorstein DB, Armstrong RB. Muscle function and protein metabolism after initiation of eccentric contraction-induced injury. J Appl Physiol 1995;79(4):1260-1270.
29. Clarkson PM, Sayers SP. Etiology of exercise-induced muscle damage. Can J Appl Physiol 1999;24(3):234-248.
30. Foidart M, Foidart JM, Engel WK. Collagen localization in normal and fibrotic human skeletal muscle. Arch Neurol 1981;38(3):152-157.

31. Chakrabarti S, Kobayashi KS, Flavell RA, Marks CB, Miyake K, Liston DR, Fowler KT, Gorelick FS, Andrews NW. Impaired membrane resealing and autoimmune myositis in synaptotagmin VII-deficient mice. J Cell Biol 2003;162(4):543-549.
32. Kornegay JN, Gorgacz EJ, Dawe DL, Bowen JM, White NA, DeBuysscher EV. Polymyositis in dogs. J Am Vet Med Assoc 1980;176(5):431-438.
33. Rosenberg NL. Neuromuscular histopathology in (New Zealand black x New Zealand white)F1 and MRL-lpr/lpr autoimmune mice: models for skeletal muscle involvement in connective tissue disease. Arthritis Rheum 1988;31(6):806-811.
34. Rosenberg NL, Ringel SP, Kotzin BL. Experimental autoimmune myositis in SJL/J mice. Clin Exp Immunol 1987;68(1):117-129.
35. Kojima T, Tanuma N, Aikawa Y, Shin T, Sasaki A, Matsumoto Y. Myosin-induced autoimmune polymyositis in the rat. J Neurol Sci 1997;151(2):141-148.
36. Willmann R, Possekel S, Dubach-Powell J, Meier T, Ruegg MA. Mammalian animal models for Duchenne muscular dystrophy. Neuromuscul Disord 2009;19(4):241-249.
37. Sunada Y, Bernier SM, Kozak CA, Yamada Y, Campbell KP. Deficiency of merosin in dystrophic dy mice and genetic linkage of laminin M chain gene to dy locus. Journal of Biological Chemistry 1994;269(19):13729-13732.
38. Miyagoe Y, Hanaoka K, Nonaka I, Hayasaka M, Nabeshima Y, Arahata K, Nabeshima Y-i, Takeda Si. Laminin [alpha]2 chain-null mutant mice by targeted disruption of the Lama2 gene: a new model of merosin (laminin 2)-deficient congenital muscular dystrophy. FEBS Letters 1997;415(1):33-39.
39. Sander M, Chavoshan B, Harris SA, Iannaccone ST, Stull JT, Thomas GD, Victor RG. Functional muscle ischemia in neuronal nitric oxide synthase-deficient skeletal muscle of children with Duchenne muscular dystrophy. Proceedings of the National Academy of Sciences of the United States of America 2000;97(25):13818-13823.
40. Adamo CM, Dai D-F, Percival JM, Minami E, Willis MS, Patrucco E, Froehner SC, Beavo JA. Sildenafil reverses cardiac dysfunction in the mdx mouse model of Duchenne muscular dystrophy. Proceedings of the National Academy of Sciences;107(44):19079-19083.
41. Lovering RM, McMillan AB, Gullapalli RP. Location of myofiber damage in skeletal muscle after lengthening contractions. Muscle & Nerve 2009;40(4):589-594.
42. Heemskerk A, Strijkers G, Drost M, van Bochove G, Nicolay K. Skeletal muscle degeneration and regeneration following femoral artery ligation in the mouse: diffusion tensor imaging monitoring. Radiology 2007;243(2):413-421.
43. Heemskerk AM, Drost MR, van Bochove GS, van Oosterhout MF, Nicolay K, Strijkers GJ. DTI-based assessment of ischemia-reperfusion in mouse skeletal muscle. Magn Reson Med 2006;56(2):272-281.
44. Mattila KT, Lukka R, Hurme T, Komu M, Alanen A, Kalimo H. Magnetic Resonance Imaging and Magnetization Transfer in Experimental Myonecrosis in the Rat. Magnetic Resonance in Medicine 1995;33(2):185-192.
45. Walter GA, Cahill KS, Huard J, Feng H, Douglas T, Sweeney HL, Bulte JWM. Noninvasive monitoring of stem cell transfer for muscle disorders. Magnetic Resonance in Medicine 2004;51(2):273-277.

46. Wishnia A, Alameddine H, Tardif de Géry S, Leroy-Willig A. Use of magnetic resonance imaging for noninvasive characterization and follow-up of an experimental injury to normal mouse muscles. Neuromuscular Disorders 2001;11(1):50-55.
47. Ababneh Z, Beloeil H, Berde CB, Gambarota G, Maier SE, Mulkern RV. Biexponential parameterization of diffusion and T_2 relaxation decay curves in a rat muscle edema model: decay curve components and water compartments. Magn Reson Med 2005;54(3):524-531.
48. Fan R, Does M. Compartmental relaxation and diffusion tensor imaging measurements in vivo in λ-carrageenan-induced edema in rat skeletal muscle. NMR in Biomed 2007;21(6):566-573.
49. Belton PS, Jackson RR, Packer KJ. Pulsed NMR studies of water in striated muscle. I. Transverse nuclear spin relaxation times and freezing effects. Biochim Biophys Acta 1972;286(1):16-25.
50. Belton PS, Packer KJ. Pulsed NMR studies of water in striated muscle. III. The effects of water content. Biochim Biophys Acta 1974;354(2):305-314.
51. Belton PS, Packer KJ, Sellwood TC. Pulsed NMR studies of water in striated muscle. II. Spin-lattice relaxation times and the dynamics of non-freezing fraction of water. Biochim Biophys Acta 1973;304(1):56-64.
52. Hazlewood CF, Chang DC, Nichols BL, Woessner DE. Nuclear magnetic resonance transverse relaxation times of water protons in skeletal muscle. Biophys J 1974;14(8):583-606.
53. Fung BM, Puon PS. Nuclear magnetic resonance transverse relaxation in muscle water. Biophys J 1981;33(1):27-37.
54. Cole WC, LeBlanc AD, Jhingran SG. The origin of biexponential T_2 relaxation in muscle water. Magn Reson Med 1993;29(1):19-24.
55. Ploutz-Snyder LL, Nyren S, Cooper TG, Potchen EJ, Meyer RA. Different effects of exercise and edema on T_2 relaxation in skeletal muscle. Magn Reson Med 1997;37(5):676-682.
56. Saab G, Marsh GD, Casselman MA, Thompson RT. Changes in human muscle transverse relaxation following short-term creatine supplementation. Exp Physiol 2002;87(3):383-389.
57. Saab G, Thompson RT, Marsh GD. Multicomponent T_2 relaxation of in vivo skeletal muscle. Magn Reson Med 1999;42(1):150-157.
58. Saab G, Thompson RT, Marsh GD. Effects of exercise on muscle transverse relaxation determined by MR imaging and in vivo relaxometry. J Appl Physiol 2000;88(1):226-233.
59. Saab G, Thompson RT, Marsh GD, Picot PA, Moran GR. Two-dimensional time correlation relaxometry of skeletal muscle in vivo at 3 Tesla. Magn Reson Med 2001;46(6):1093-1098.
60. Radhakrishnan R, Moore SA, Sluka KA. Unilateral carrageenan injection into muscle or joint induces chronic bilateral hyperalgesia in rats. Pain 2003;104(3):567-577.
61. McIntosh LM, Baker RE, Anderson JE. Magnetic resonance imaging of regenerating and dystrophic mouse muscle. Biochem Cell Biol 1998;76(2-3):532-541.

62. Walter G, Cordier L, Bloy D, Lee Sweeney H. Noninvasive monitoring of gene correction in dystrophic muscle. Magnetic Resonance in Medicine 2005;54(6):1369-1376.
63. Parchen C, Gray H, Percival J, Froehner S, Beavo JA. Effect of sildenafil on mdx skeletal muscle. 2008; San Diego, CA. p 1137.1113.
64. Cleveland GG, Chang DC, Hazlewood CF, Rorschach HE. Nuclear magnetic resonance measurement of skeletal muscle: anisotropy of the diffusion coefficient of the intracellular water. Biophys J 1976;16(9):1043-1053.
65. Basser PJ, Mattiello J, LeBihan D. MR diffusion tensor spectroscopy and imaging. Biophys J 1994;66(1):259-267.
66. Jones DK, Cercignani M. Twenty-five pitfalls in the analysis of diffusion MRI data. NMR in Biomedicine;23(7):803-820.
67. Damon BM, Ding Z, Anderson AW, Freyer AS, Gore JC. Validation of diffusion tensor MRI-based muscle fiber tracking. Magn Reson Med 2002;48(1):97-104.
68. Lansdown DA, Ding Z, Wadington M, Hornberger JL, Damon BM. Quantitative diffusion tensor MRI-based fiber tracking of human skeletal muscle. J Appl Physiol 2007;103(2):673-681.
69. Sinha S, Sinha U, Edgerton VR. In vivo diffusion tensor imaging of the human calf muscle. J Magn Reson Imaging 2006;24(1):182-190.
70. Tanner JE. Self diffusion of water in frog muscle. Biophys J 1979;28(1):107-116.
71. Kim S, Chi-Fishman G, Barnett AS, Pierpaoli C. Dependence on diffusion time of apparent diffusion tensor of ex vivo calf tongue and heart. Magn Reson Med 2005;54(6):1387-1396.
72. Vajda Z, Pedersen M, Doczi T, Sulyok E, Nielsen S. Studies of mdx mice. Neuroscience 2004;129(4):993-998.
73. McMillan AB, Ward CW, Lovering RM. Assessment of skeletal muscle damage in mice using diffusion tensor MRI. American College of Sports Medicine Annual Meeting, 2010. Baltimore, MD.
74. Straub V, Donahue KM, Allamand V, Davisson RL, Kim YR, Campbell KP. Contrast agent-enhanced magnetic resonance imaging of skeletal muscle damage in animal models of muscular dystrophy. Magnetic Resonance in Medicine 2000;44(4):655-659.